

## Chopper-Stabilized Amplifiers With a Track-and-Hold Signal Demodulator

By Alberto Bilotti, Life Senior Member, IEEE,  
and Gerardo Monreal

**Abstract**—The conventional signal demodulator of a chopper amplifier can be substituted by track-and-hold (T/H) and averaging functions. This arrangement provides offset cancellation without requiring low-pass filters and can ignore the residual offset generated by input spikes. A noise analysis shows that this T/H demodulator degrades the white noise signal-to-noise ratio (SNR), although degradation can be minimized by using maximum duty cycle and minimum amplifier bandwidth.

**Index Terms**—Broadband white noise semiconductor, chopper amplifiers, offset cancellation, track and hold demodulator.

### I. INTRODUCTION

The chopper stabilization of amplifiers is a well-known technique for reducing the input direct current (DC) offset and low-frequency input noise that usually degrades the performance of precision DC amplifiers [1]–[3]. Fig. 1 shows the basic principle.

The input signal is first multiplied by a unit symmetrical square wave function  $S1(t)$  of frequency  $f_{clk}$ , then amplified by an amplifier of gain  $G$ , multiplied again by a switching function  $S2(t)$  similar to  $S1(t)$ , and finally low-pass filtered. The first multiplication translates the input signal spectrum into the high-frequency (HF) region and the second recovers the amplified original signal by demodulating the signal back to the base band. On the other hand the input-referred amplifier DC offset and low-frequency noise components go only through the second multiplication process. The DC offset, for example, being converted into an HF square wave function that is fully attenuated by the low-pass filter. The multiplication functions are usually implemented by simple pairs of metal-oxide-semiconductor (MOS) switches controlled by the CLK signal.

A problem of the conventional chopper lies in the possible generation of parasitic offsets due to the first multiplication switching transients, these offsets going through the

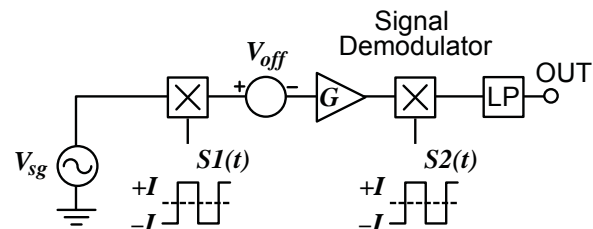


Fig. 1. Conventional chopper-stabilized amplifier.

low-pass filter uncancelled. Another problem is the low-pass filtering required for attenuating the residual square wave ripple due to the offset. This is particularly severe in monolithic choppers where multiple-pole low-pass (LP) filters require an appreciable silicon area.

We describe next the pros and cons of replacing the conventional signal demodulator by a track-and-hold (T/H)-based demodulator.

### II. THE TRACK-AND- HOLD SIGNAL DEMODULATOR

Let us assume that the input signal to the chopper-stabilized amplifier  $Vsg$  is bandwidth limited to the Nyquist frequency ( $f_{clk}/2$ ) and that the amplifier is noiseless.

The residual offset due to input switching transient spikes which are short as compared to  $T_{clk}/2$  can be reduced appreciably by narrowbanding the amplifier as much as possible [2] or including a bandpass filter with center frequency locked to  $f_{clk}$  [4]. In cases where the chopper operates at relatively higher frequencies and the input spikes duration is no longer negligible as compared to  $T_{clk}/2$ , similar results can be achieved by widebanding the amplifier and making  $S2(t)$  a switching function with a lower than 50% duty cycle, as shown in Fig. 2, such that during  $\Delta t$  intervals, where the

amplified spikes lie, the output is zero. This technique introduces a signal attenuation given by  $\Delta t / (T_{clk}/2)$  and a larger white noise.

The signal attenuation can be avoided and the LP filter requirements relaxed when a holding function is appropriately included in the signal demodulator. For example, Fig. 3 shows a signal demodulator comprising a two-T/H plus an adder (or averaging) arrangement that could be used instead of the conventional signal demodulator of Fig. 1.

The T/H inputs are the noninverted and inverted amplified chopped signals, while the T/H outputs are applied to the adder. The T/H switches are closed by pulses occurring during the CLK and the  $\overline{CLK}$  timing signals with duty cycle  $d$ . We assume that the chopped signal goes through the amplifier without distortion, which means amplifier bandwidths five or more times the  $f_{clk}$ .

With this arrangement, assuming ideal switches and zero offset, and recalling that the chopped signal changes sign at each CLK half cycle, each T/H recovers the original signal  $G \times V_{sg}$  and the adder generates a  $2G \times V_{sg}$  output which is updated each CLK half cycle.

As far as the DC offset (or the low frequency noise components) is concerned the offset, being not chopped, does not change sign at each CLK half cycle and therefore the T/H outputs are DC voltages with opposite polarities, the offset being cancelled by the adder.

The advantages of this signal demodulator for a chopper-stabilized amplifier can be summarized as follows:

- The offset is cancelled without requiring any LP filtering. Any residual offset is only due to T/H mismatches and adder inaccuracies.
- Due to the interlaced sampling, the typical staircase ripple associated to the output waveform has a  $2f_{clk}$  fundamental frequency, which simplifies its removal.
- Residual offsets due to input switching transients can be removed, if desired, by proper relative phrasing of the tracking pulses without an attenuation penalty.
- A signal conditioner using a chopper amplifier with a T/H signal demodulator for cancelling the relatively large offsets occurring in a switched-Hall magnetic sensor was recently reported [5].

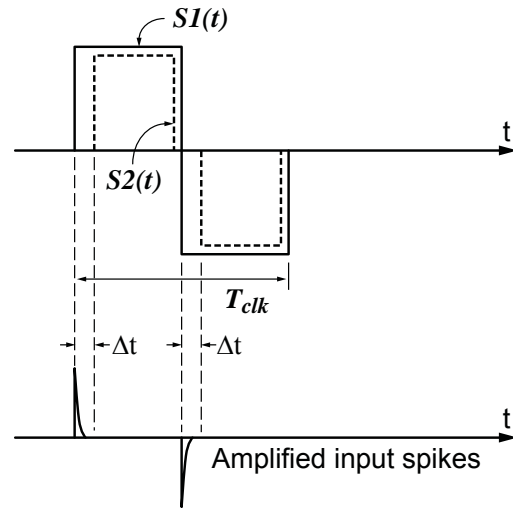


Fig. 2. Input spike removal by proper shaping of the second multiplier switching function.

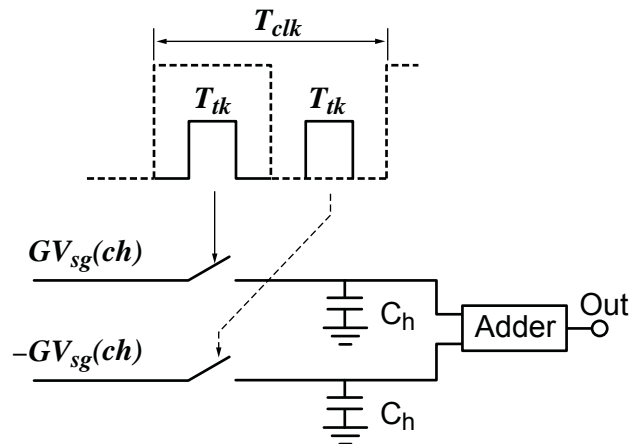


Fig. 3. T/H demodulator.

Fig. 4 shows a fully differential chopper using the previously described T/H signal demodulator. Switches  $SW_i$ , driven by a square-wave 5-V clock signal  $CLK1$  perform the first multiplication, while switches  $SW1$  and  $SW2$ , driven by sampling pulses  $CLK2$  and  $CLK3$  together with  $C1$  and  $C2$  and averaging resistors  $R1$  and  $R2$ , make up the T/H signal demodulator. A similar T/H demodulator, fed from the amplifier output but with reverse polarity, has been included in order to generate a fully differential output. The T/H switches are complementary MOS (CMOS) pass transistors, while the input switches are simple N-channel pass transistors in order to intentionally enhance the amplitude of the input transient spikes. The amplifier, with a gain of  $40\times$  and a 3-dB bandwidth of 3 MHz, is assumed ideal, its offset being

simulated with an input DC generator  $V_{off}$ . Fig. 4 also shows the  $CLK$  waveforms, the sampling pulses  $CLK2$  and  $CLK3$  occurring approximately at the center of the  $CLK1$  half cycles.

A SPICE simulation of the circuit of Fig. 4 was performed for  $f_{clk} = 160$  kHz,  $d = T_{tk}/T_{clk} = 0.25$ , a 5-kHz sinusoidal input signal of 0.5-mV amplitude, and a DC input offset of 5 mV. The SPICE model parameters for all devices were derived from a standard 2- $\mu$  mixed bipolar CMOS (BiCMOS) process.

Fig. 5(a) shows the input signal plus the amplifier DC offset waveforms and Fig. 5(b) the voltage waveform at the amplifier output prior to the T/H demodulator. Although the chopped signal appears embedded in relatively large transient pulses, the

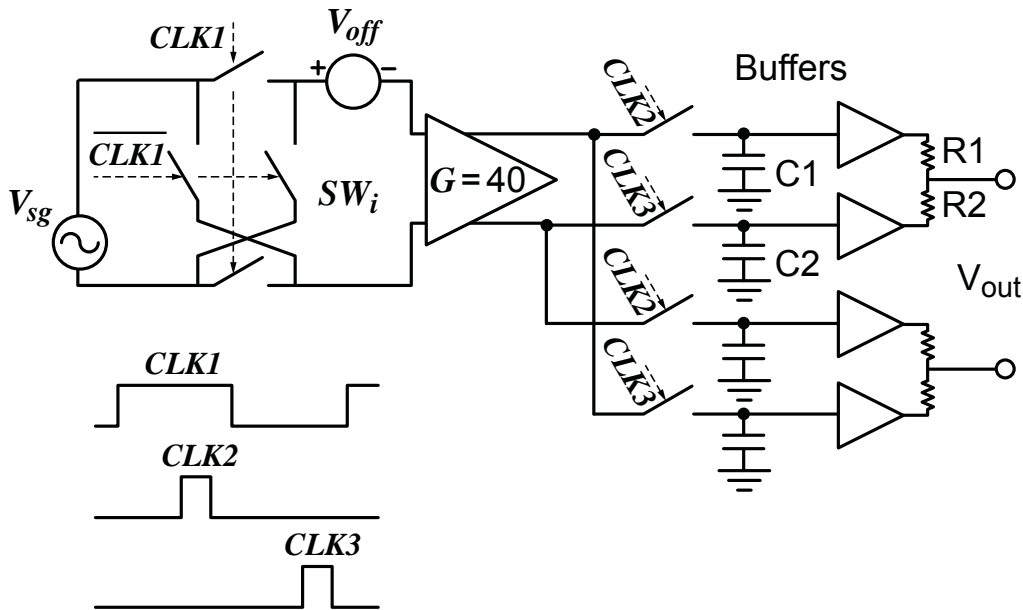


Fig. 4. Fully differential chopper using a T/H signal demodulator.

appropriate relative phasing of the sampling pulses allows clean recovering of the original signal waveform, as shown in the output voltage waveform of Fig. 5(c).

The output voltage is an amplified replica of the input signal except for the quasi-staircase ripple typical of the sample and

hold (S/H) functions. As in all sample-data systems, as the signal frequency approaches the Nyquist frequency  $f_{clk}/2$ , the residual staircase ripple becomes more relevant and a postchopper LP filter may be required for recovering the undistorted waveform. For example, Fig. 6(a) shows the same output waveform as in Fig. 5(c), but with the chopper operating at a signal frequency

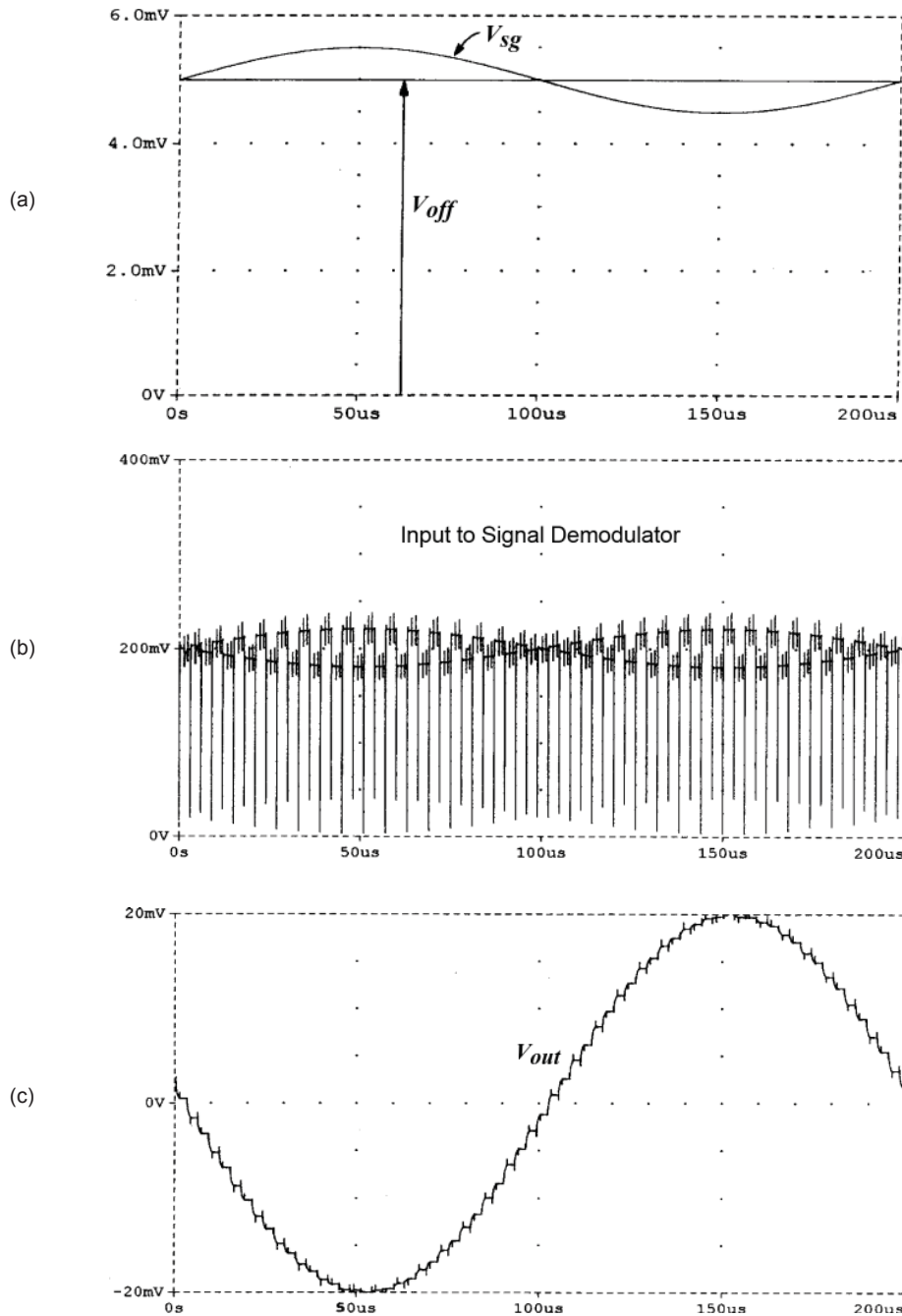


Fig. 5. SPICE simulation of the chopper of Fig. 4. (a) Input signal and input DC offset. (b) Amplifier output voltage waveform, prior to the T/H demodulator. (c) Output voltage.

of 30 kHz, i.e., at  $\approx 0.4(f_{\text{clk}}/2)$  the output waveform appearing severely distorted due to the excessive staircase ripple. Fig. 6(b) shows how the original waveform can be approximately recovered by using a postchopper one-pole LP filter with a  $-3\text{-dB}$  frequency of 60 kHz.

### III. INPUT-REFERRED OFFSET

In the real circuit, the offset cancellation is mainly limited by mismatches in the demodulator. If  $V_{oi_a}$  is the amplifier input-referred offset, any relative mismatch  $M = \Delta R/R$  between resistors R1 and R2 in the adder of Fig. 4 will generate an input-

referred offset  $M \times V_{oi_a}$  in the chopper, while an equivalent offset  $V_{ob}$  due to T/H and buffer imbalances will generate an input-referred offset  $V_{ob}/G$ . Assuming the residual offset due to input spikes has been removed, and that all imbalances and offsets are statistically independent random function with Gaussian distribution and zero-mean value, we can write for the chopper input-referred offset  $V_{oi_{ch}}$

$$\sigma(V_{oi_{ch}}) = \left\{ [\sigma(M) \cdot \sigma(V_{oi_a})]^2 + \left[ \frac{\sigma(V_{ob})}{G} \right]^2 \right\}^{1/2} \quad (1)$$

where  $\sigma(x)$  is the standard deviation of  $x$  and  $G$  the amplifier gain.

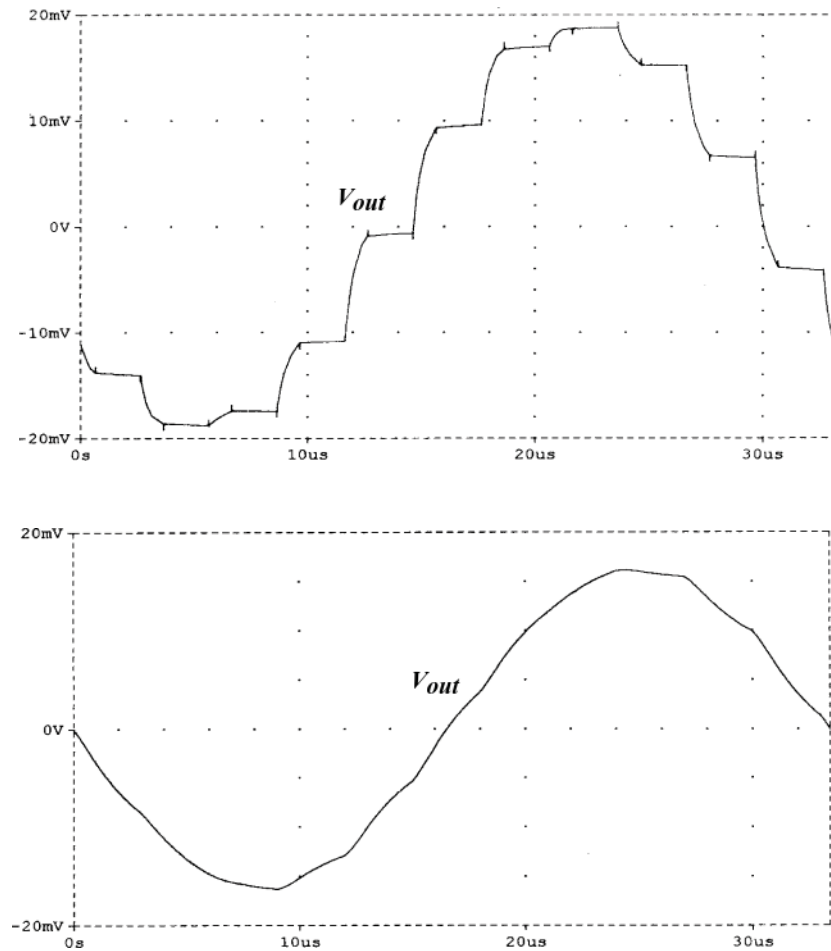


Fig. 6. Output waveforms similar to Fig. 5(c) but with the chopper amplifier of Fig. 4 operating with  $f_{\text{sg}} = 30$  kHz. (a) Without any LP filtering. (b) With a postchopper one-pole LP filter with a  $-3\text{-dB}$  frequency of 60 kHz.

Expression (1) shows that, depending on the demodulator imbalances and the amplifier input-referred offset, there is not much to be gained by increasing excessively the amplifier gain.

As in conventional choppers, asymmetries in the amplifier DC transfer characteristics can also limit the offset cancellation by introducing differences between the noninverted and inverted amplified chopped signals. Generally, the use of well-matched differential amplifiers makes this source of error negligible as compared to those given in equation 1.

Besides, the addition of holding functions and the use of an amplifier with a bandwidth much larger than the clock frequency, degrades the signal-to-noise ratio (SNR) of this type of demodulator, as will be shown in the next section.

#### IV. NOISE CONSIDERATIONS

In all practical cases, a white-noise voltage, due to the amplifier input-referred white-noise voltage, amplified  $G$  times and limited by the amplifier bandwidth, appears at the input of each S/H in the demodulator of Fig. 2.

Let us first analyze the white-noise behavior in one simple T/H. Assume a white-noise voltage with an ideal rectangular noise spectrum of bandwidth  $BW_n$  and power spectrum density  $\eta_i$  is applied to the input of a T/H and call  $\eta_o$  the noise power spectrum density at the T/H output. As was previously mentioned for avoiding distortion of chopped signals, the amplifier bandwidth must be much larger than  $f_{clk}$ , therefore  $BW_n \gg f_{clk}$  and the noise is undersampled by the T/H switch.

The noise generated by the tracking pulses of length  $d \times T_{clk}$  do not increase appreciably the output noise, but during the hold time  $(1-d)T_{clk}$  additional noise is introduced due to fold over of all high-frequency (HF) noise components modulated around the clock frequency harmonics into the base band, making  $\eta_o > \eta_i$ . This aliasing occurs because the periodic hold behaves as an equivalent ideal S/H function where appreciable aliasing occurs whenever the input spectrum extends over the Nyquist band [6]–[8].

The white-noise transfer function of an ideal T/H has been analyzed by Fischer [6], assuming that the output noise power spectral density is the sum of the noise power generated during the track interval, plus the noise power generated during the hold interval. Focusing our interest on the range  $0 < f < f_{clk}/2$  and recalling expressions A2, B5a and B5b of [6] we can write a

general expression for the noise power spectral density transfer function of a simple T/H, as follows:

$$\left[ \frac{\eta_o}{\eta_i} \right]_{f < \frac{f_{clk}}{2}} = d^2 \cdot \left[ 1 + 2 \cdot \sum_{n=1}^h \text{sinc}^2(n \cdot d) \right] + (1-d)^2 \cdot (1+2 \cdot h) \cdot \text{sinc}^2 \left[ (1-d) \cdot \frac{f}{f_{clk}} \right] \quad (2)$$

where the first and second terms represent the track and hold contributions, respectively,  $\eta_i$  and  $\eta_o$  are the input and output noise spectral power densities and

$d$  is the duty cycle ( $T_{tk}/T_{clk}$ ),

$f_{clk}$  is  $1/T_{clk}$  = clock frequency,

$h$  is the closest integer to the  $BW_n/f_{clk}$  ratio, and

$\text{sinc}(x)$  is  $[\sin(\pi \times x)]/\pi \times x$ .

Note that for  $d = 0$  there is a pure S/H function with  $\eta_o/\eta_i = (1 + 2 \times h) \times \text{sinc}^2(f/f_{clk})$  while for  $d = 1$  there is no S/H, the tracking switch being permanently on, with  $\eta_o/\eta_i = 1$ . When parameter  $h$  is zero there is no aliasing as the noise input spectrum remains below  $f_{clk}/2$ . When  $h = 1, 2, 3$ , etc., there is additional noise due to the input noise spectrum going beyond  $f_{clk}/2$  reaching the first, second, third, etc., CLK harmonics and folding back into the Nyquist band. As the output noise spectrum is approximately flat within the Nyquist band, equation 2 can be simplified assuming the worst case of a constant power spectral density equal to the maximum value occurring at  $f = 0$ . Thus:

$$\left[ \frac{\eta_o}{\eta_i} \right]_{f < \frac{f_{clk}}{2}} = d^2 \cdot \left[ 1 + 2 \cdot \sum_{n=1}^h \text{sinc}^2(n \cdot d) \right] + (1-d)^2 \cdot (1+2 \cdot h) \quad (3)$$

Equation 3, giving the white noise degradation in the Nyquist band for a simple T/H function, has been plotted in Fig. 7 in the range  $0 < d < 1$  and for various values of  $h$ . As expected, the noise degradation is maximum for  $d = 0$  and increases with increasing  $h$ .

Going back to the demodulator of Fig. 3, the noise outputs of the two T/Hs, each one fed by the same noise voltage but with inverted polarities, are added. For the low-frequency region of the noise input spectrum involving frequencies much smaller than

$f_{\text{clk}}$ , the T/H output noise voltages are correlated and therefore cancel out. This cancellation action includes the DC offset voltage and the relatively low-frequency  $1/f$  noise. For the rest of the input noise spectrum up to  $BW_n$ , where most of the noise voltages become uncorrelated and their power spectral densities are directly summed up by the adder.

Thus, with the initial assumption  $BW_n \gg f_{\text{clk}}$  we can assume that practically all the white-noise voltages generated at the two T/H outputs are due to aliasing and therefore uncorrelated; the demodulator of Fig. 3 showing a worst case output noise power spectral density  $\approx 2\eta_o$ . As the output signal power is four times the input signal power, the demodulator noise figure (NF), as far as the white noise is concerned, becomes:

$$NF = \frac{(S/N)_i}{(S/N)_o} = \frac{1}{2} \cdot \frac{\eta_o}{\eta_i} \quad (4)$$

where  $\eta_o/\eta_i$  refers to the noise power spectrum density transfer function of a single T/H for  $f < f_{\text{clk}}/2$  (Fig. 7).

For example, for  $d = 0.3$  and  $h = 5$ , the  $\eta_o/\eta_i$  ratio from Fig. 7 is six and the noise figure of the signal demodulator three. As the tracking pulse width cannot be higher than one clock half cycle, the maximum allowable duty cycle is 0.5 and Fig. 7 shows that

the noise due to aliasing is the dominant contributor to the T/H demodulator noise.

## V. CONCLUSION

The performance of a chopper-stabilized amplifier where the signal demodulation or second multiplication function is performed by a double T/H and adder arrangement has been described. The most important advantage of this approach, as compared to the conventional chopper, consists in the cancellation of the amplifier input offset, low-frequency input noise components, and residual offsets due to input switching spikes, without requiring any low-pass filtering. The maximum offset cancellation achievable is limited by the T/H mismatches and by the adder accuracy.

For avoiding excessive staircase ripple on the output waveform, the input signal spectrum bandwidth should be preferably smaller than 0.2 times the Nyquist frequency. Otherwise a postchopper LP filter may be required.

Finally, these demodulators show a white-noise degradation due to the hold function; this degradation being minimum for the maximum allowable duty cycle of 0.5 and minimum amplifier bandwidth.

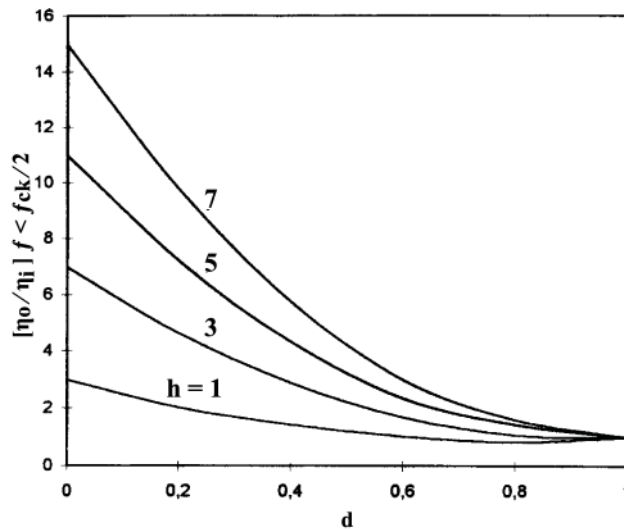


Fig. 7. White-noise power spectral density transfer function of a simple T/H for  $f < f_{\text{clk}}/2$ , where  $d$  is the track pulse duty cycle and  $h$  the closest integer to  $BW_n/f_{\text{clk}}$ , and where the worst case occurring at  $f = 0$  was assumed.

---

## ACKNOWLEDGMENT

The authors would like to thank D. Barrettino, of Electrónica Bilotti, for his helpful suggestions.

## REFERENCES

- [1] K. Hsieh et al., "A low-noise chopper stabilized differential switched-capacitor filtering technique," *IEEE J. Solid-State Circuits*, vol. SC-16, no. 6, pp. 708-715, Dec. 1981.
- [2] C. C. Enz et al., "A CMOS chopper amplifier," *IEEE J. Solid-State Circuits*, vol. SC-22, pp. 335-341, June 1987.
- [3] C. C. Enz and G. C. Temes, "Circuit techniques for reducing the effects of op-amp imperfections: Autozeroing, correlated double sampling, and chopper stabilization," *Proc. IEEE*, vol. 84, pp. 1584-1613, Nov. 1996.
- [4] C. Menolfi and Q. Huang, "A low-noise CMOS instrumentation amplifier for thermoelectric infrared detectors," *IEEE J. Solid-State Circuits*, vol. 32, pp. 968-976, July 1997.
- [5] A. Bilotti et al., "Monolithic magnetic hall sensor using dynamic quadrature offset cancellation," *IEEE J. Solid-State Circuits*, vol. 32, pp. 829-836, June 1997.
- [6] J. S. Fischer, "Noise sources and calculation techniques for switched capacitor filters," *IEEE J. Solid-State Circuits*, vol. SC-17, pp. 742-752, Aug. 1982.
- [7] C. Gobet, "Spectral distribution of a sampled first order lowpass filtered white noise," *Electron. Lett.*, vol. 17, no. 19, pp. 720-721, Sept. 1981.
- [8] C. Gobet and A. Knob, "Noise analysis of switched capacitor networks," *IEEE Trans. Circuits Syst.*, vol. CAS-30, pp. 37-43, Jan. 1983.

Manuscript received November 10, 1997; revised May 2, 1998.  
This work was supported by Allegro™ MicroSystems, LLC. This paper was recommended by Associate Editor M. Biey.

A. Bilotti is with Electrónica Bilotti, Olivos 1636, Argentina.

G. Monreal is with Sensor Development Group, Allegro™ MicroSystems, LLC, Concord, NH 03306 USA.

Publisher Item Identifier S 1057-7122(99)02748-8.

The signal demodulator described here is incorporated into the A3150, A3210, A3240, A3260, A3280, A3361, and A3515 Hall-effect sensor ICs.

1057-7122/99\$10.00 © 1999, IEEE

The information contained in this document does not constitute any representation, warranty, assurance, guaranty, or inducement by Allegro to the customer with respect to the subject matter of this document. The information being provided does not guarantee that a process based on this information will be reliable, or that Allegro has explored all of the possible failure modes. It is the customer's responsibility to do sufficient qualification testing of the final product to insure that it is reliable and meets all design requirements.